Supporting information

$ZnIn_2S_4$ Combined with a Flower-like NiAl-layered Double Hydroxide with Enhanced Photocatalytic H_2 Production Activity

Anna P. Souri[1,2] , Onur Cavdar[2] , Maria Zografaki[1,3] , Leila Zouridi[1,4] , Vassilios Binas[1,3] , Tomasz Klimczuk[5,6], Kostiantyn Nikiforow[7], Anna Malankowska[2*]

[1] Institute of Electronic Structure and Laser, Foundation for Research and Technology-Hellas, 71110 Heraklion,
[2] Department of Environmental Technology, Faculty of Chemistry, University of Gdansk, 80-308 Gdansk, Poland
[3] Department of Chemistry, Aristotle University of Thessaloniki, Thessaloniki, Greece
[4] Department of Materials Science and Technology, University of Crete, Heraklion, Greece
[5] Faculty of Applied Physics and Mathematics, Gdansk University of Technology, Narutowicza, Gdansk, Poland
[6] Advanced Materials Center, Gdansk University of Technology, Narutowicza, Gdansk, Poland
[7] Mazovia Center for Surface Analysis, Institute of Physical Chemistry, Polish Academy of Sciences, 01-224, Warsaw, Poland
*anna.malankowska@ug.edu.pl

Table S1: Reports of ZIS/LDHs pairing from literature

Reference	Composite	Application	H_2 rate (mmol $g^{-1}h^{-1}$)	Irradiation	AQE (%)	λ (nm)
Our work	ZIS/NiAl/Pt	H_2 evolution	1.6 0.3	UV-vis visible	1.7	320
[2]	ZIS/NiAl/carbon q.d.	H_2 evolution	23.1	visible	3.6	420
[3]	ZIS/NiFe	H_2 evolution	2.0	visible	7.2	420
[4]	ZIS/MgAl	Cr(VI) reduction and H_2 evolution	1.9	visible	35.7	380
[5]	ZIS/CoAl	H_2 evolution	1.5	simulated sunlight	1.5	420
[6]	NiCo/ZIS	Cr(VI) reduction		visible		
[7]	ZIS/CoAl	H_2 evolution	1.2	visible	0.6	450
[8]	NiCoFe/ZIS	H_2 evolution coupled with benzylamine oxidation	113.5	visible	14.3	420
[9]	CoNi/ZIS	tetracycline degradation under photocatalytic-peroxymonosulfate activation system				

Calculations for Pt photodeposition

In the case of ZIS/NiAl25/2.6Pt, 273 μL of $H_2PtCl_6{\cdot}6H_2O$ solution (50 mM) were dissolved in an aqueous solution (10 mL) containing 20% (v/v) methanol under vigorous stirring. The amount of $H_2PtCl_6{\cdot}6H_2O$ solution was determined by taking into consideration the percentage of Pt in the metal salt (37%) and the formula:

$$V = \frac{m}{MW\ C} \qquad (1)$$

where:

m is the amount of salt that corresponds to 2.6 wt% Pt,

MW is the molecular weight of the metal salt (517.72 gr mol^{-1}),

C is the concentration of the metal solution (50 mM).

Action spectra analysis for photocatalytic hydrogen evolution reaction

The quantum efficiency was calculated using the following equation (**Eq. 1**)

$$AQE\ (\%) = \frac{2\ x\ Number\ of\ the\ hydrogen\ molecules}{Number\ of\ the\ incident\ photons} \qquad \textbf{(Eq. 1)}$$

The derivation of the AQE formula was clearly given by Kalisman et al. [1].

Specifically, the AQE was calculated using the following formula:

$$AQE\ (\%) = \frac{2\ x\ NH2\ x\ F\ x\ 100}{P\ x\ t\ x\ A\ x\ \lambda/(h\ x\ c)} \qquad \textbf{(Eq. 2)}$$

$\mathbf{N_{H2}}$: number of moles of H_2 evolved (mol)

F: Avogadro's numer

P: is the power density of the incident light

t: irradiation time

A: is the effective illuminated area

λ: wavelength of monochromatic light

h: Planck's constant

c: speed of light

The key parameters used:

- Speed of light (c): 3×10^8 m/s
- Planck's constant (h): 6.626×10^{-34} J·s
- Avogadro's number: 6.022×10^{23} mol^{-1}
- Sensor area: 0.709 cm^2
- Irradiated area of the reactor: 3.0 cm^2
- Wavelength (λ): [provided per measurement see Fig.S1]

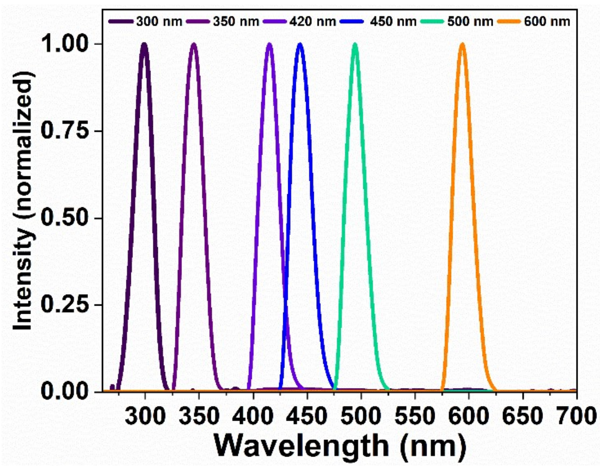

Figure S1: The emission spectra of each wavelength

(a)

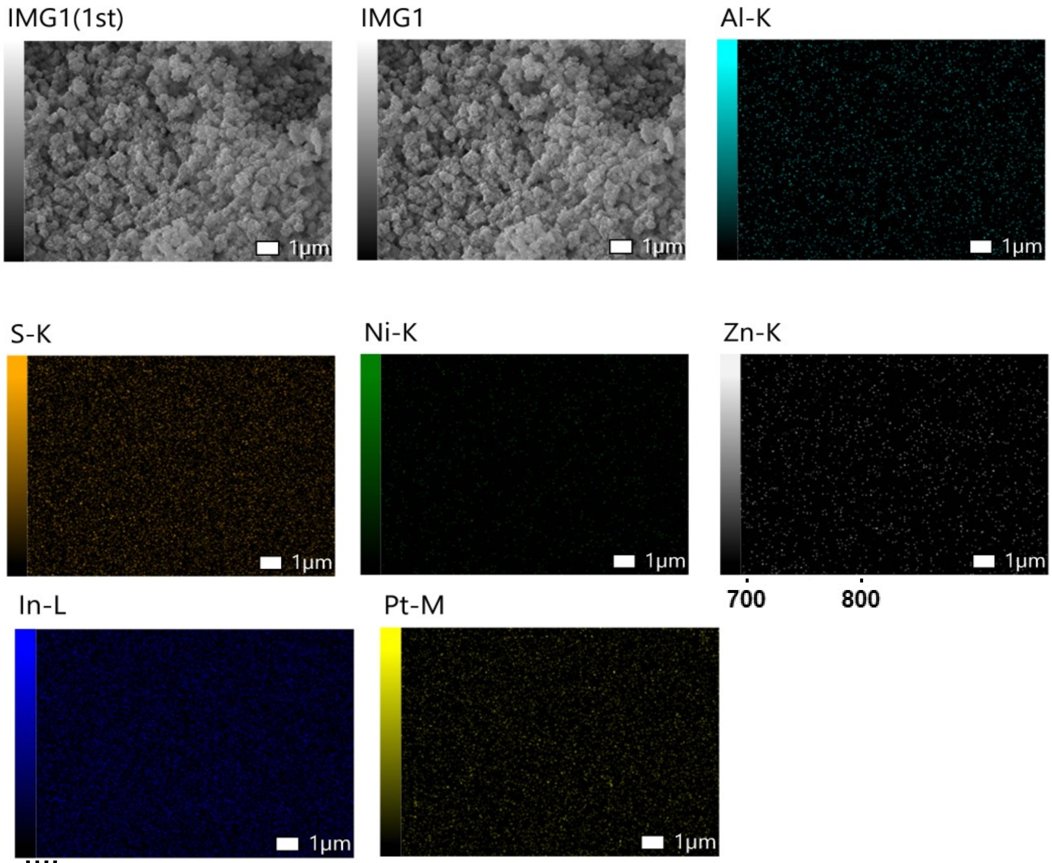

IMG1(1st)
IMG1
Al-K
S-K
Ni-K
Zn-K
In-L
Pt-M
1μm
700
800

(b)

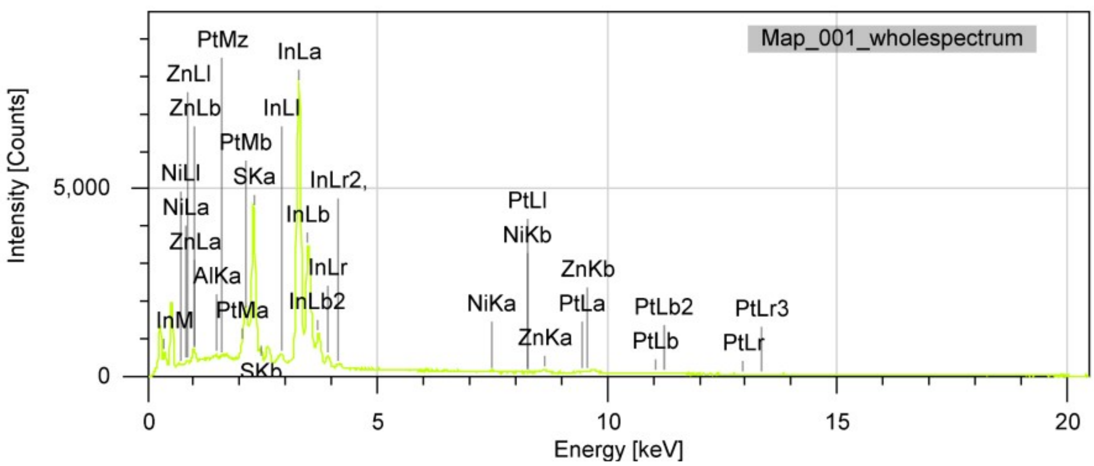

Map_001_wholespectrum
Intensity [Counts]
Energy [keV]
5,000
0
0
5
10
15
20
PtMz
InLa
ZnLl
ZnLb
InLl
PtMb
NiLl
SKa
InLr2,
NiLa
InLb
ZnLa
InLr
AlKa
InLb2
InM
PtMa
SKb
PtLl
NiKb
ZnKb
NiKa
PtLa
PtLb2
PtLr3
ZnKa
PtLb
PtLr

Figure S2: (a) Elemental mapping and (b) EDX spectrum of ZIS/NiAl25/1.95Pt sample

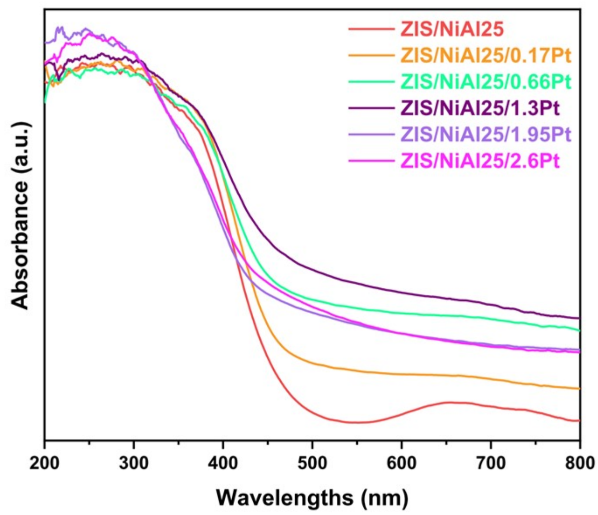

Figure S3: DRS spectra of ZIS/NiAl25 composite with different Pt loadings

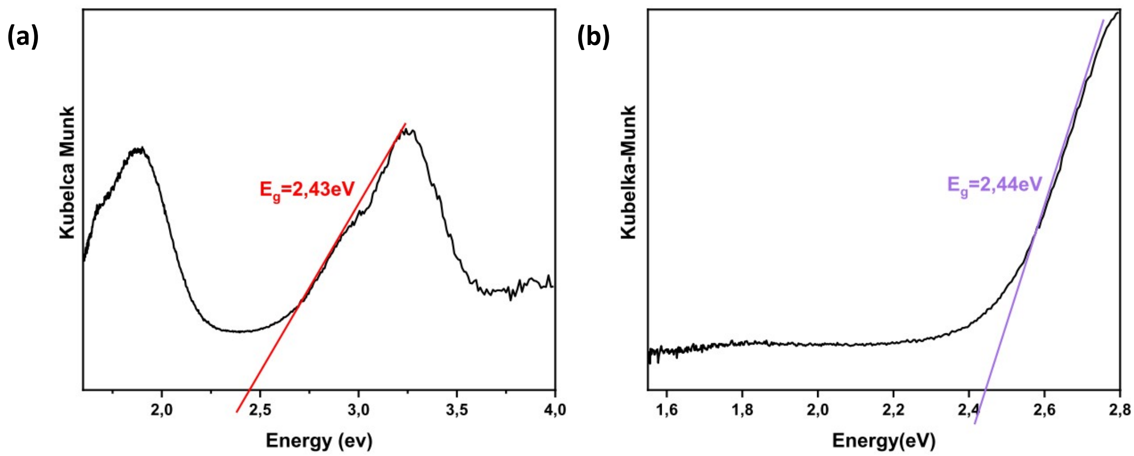

Figure S4: Tauc plots of pristine (a) NiAl and (b) ZIS and from which the Eg was extracted. The axes are (F(R)·hν)1/n- hν, where F(R) is the absorbance coefficient, hν is the photon energy (h is the Planck constant and ν is the light frequency)and n was chosen 2 for ZIS and ½ for NiAl.

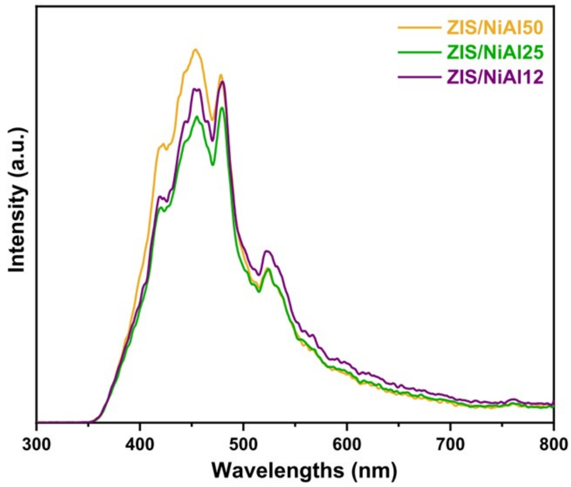

Figure S5: PL spectra of ZIS/NiAlx heterostructures where x=12.5, 25 and 50

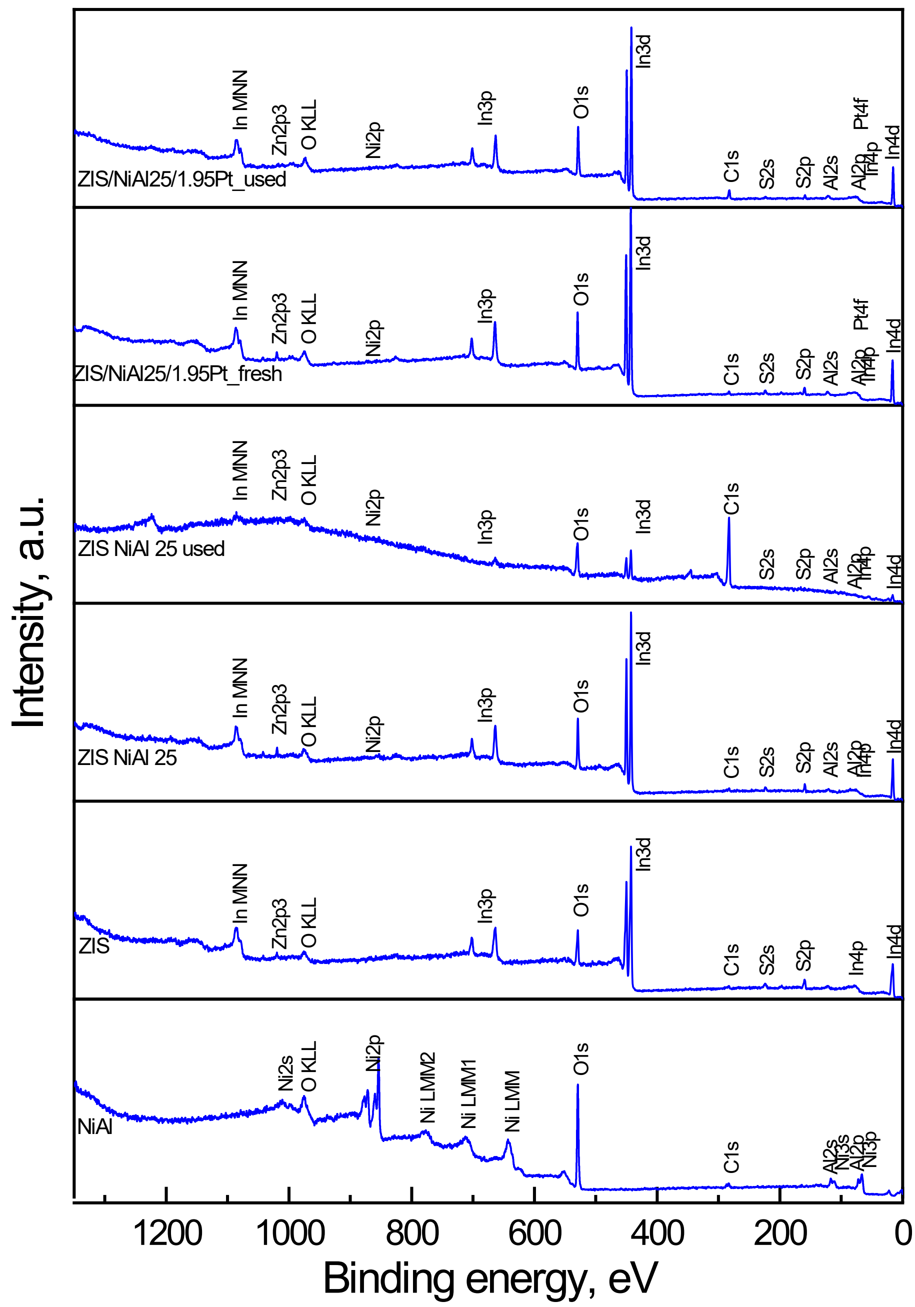

Figure S6: XPS spectra of prepared photocatalysts NiAl, ZIS, ZIS/NiAl25, ZIS/NiAl25/1.95Pt as well as ZIS/NiAl25 and ZIS/NiAl25/1.95Pt after photocatalytic reaction (marked as used)

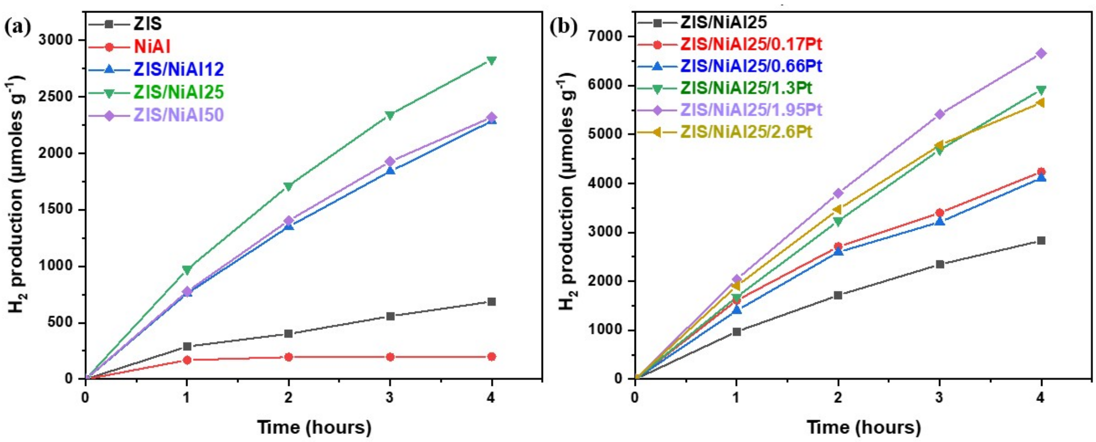

Figure S7: (a) Optimization of NiAl amount in ZIS/NiAl heterostructure and **(b)** optimization of Pt loading on ZIS/NiAl25 sample under UV-Vis irradiation. Reaction conditions: 25mg of catalyst, 20mL aqueous solution, 10% v/v of sacrificial agent (TEOA), Xe lamp 1000Watt

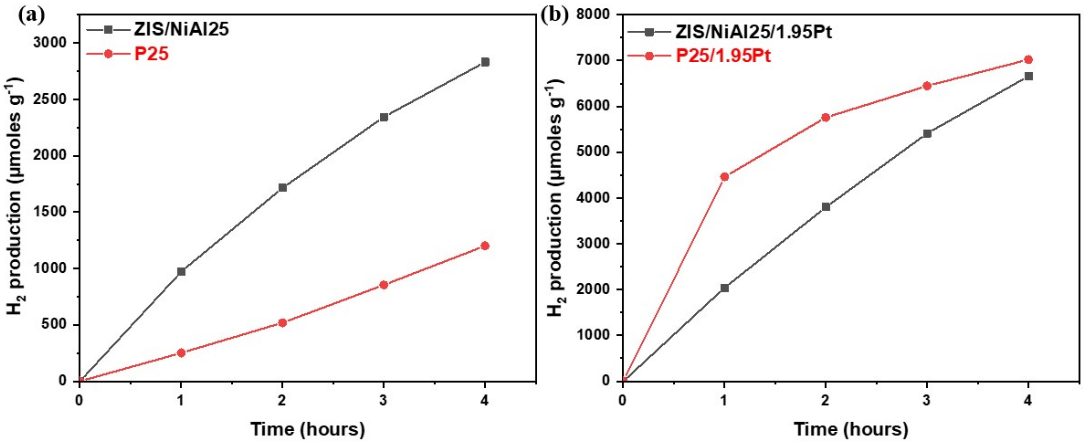

Figure S8: Comparison study **(a)** of sample with optimum NiAl amount (ZIS/NiAl 25) with P25 and **(b)** of sample with optimum Pt loading (1.95% wt) with P25 with the same Pt loading in UV-Vis irradiation. Reaction conditions: 25mg of catalyst, 20mL aqueous solution, 10% v/v of sacrificial agent (TEOA), Xe lamp 1000Watt

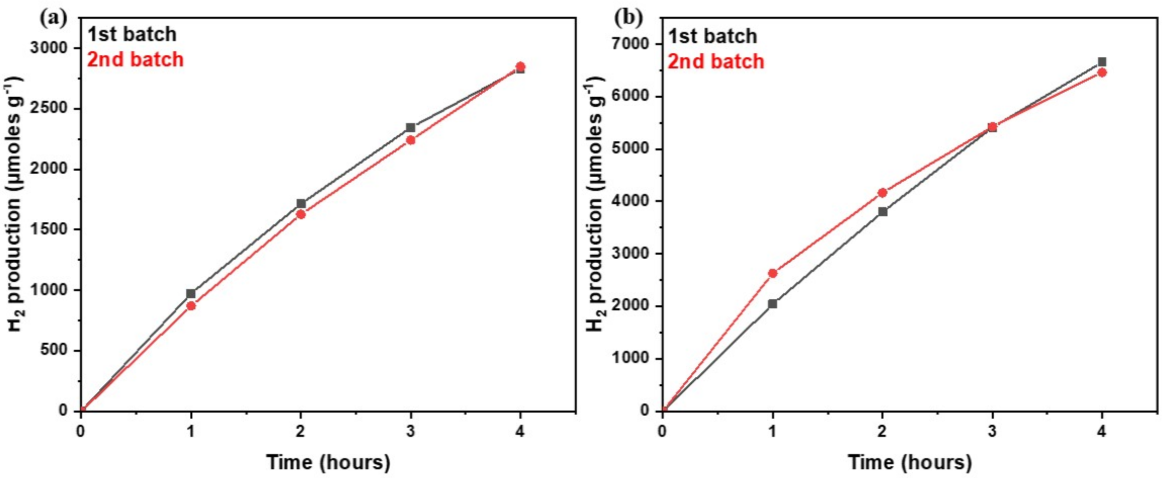

Figure S9: Photocatalytic H_2 rate of different batches of a) ZIS/NiAl25 sample and b) ZIS/NiAl25/1.95Pt sample in UV-Vis. Reaction conditions: 25mg of catalyst, 20mL aqueous solution, 10% v/v of sacrificial agent (TEOA), Xe lamp 1000Watt

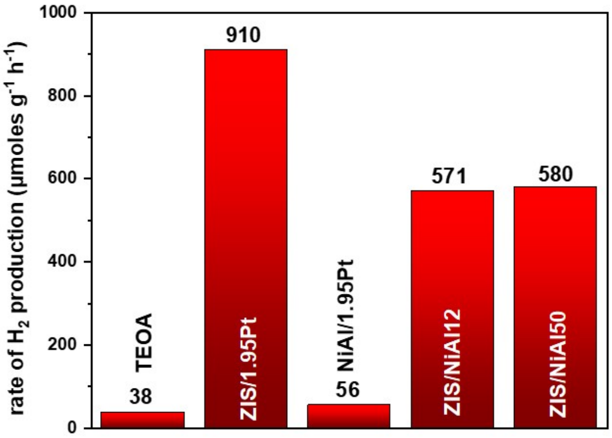

Figure S10: Photocatalytic H_2 rate of TEOA, ZIS/1.95Pt, NiAl/1.95Pt, ZIS/NiAl12 and ZIS/NiAl50 under UV-Vis. Reaction conditions: 25 mg of catalyst, 20 mL aqueous solution, 10% v/v of sacrificial agent (TEOA), Xe lamp 1000Watt

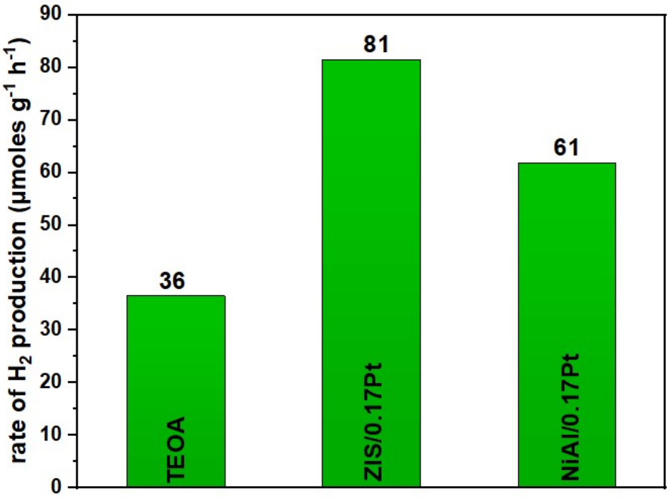

Figure S11: Photocatalytic H_2 rate of TEOA, ZIS/0.17Pt, NiAl/0.17Pt under visible irradiation (λ>420 nm). Reaction conditions: 25 mg of catalyst, 20 mL aqueous solution, 10% v/v of sacrificial agent (TEOA), Xe lamp 1000Watt

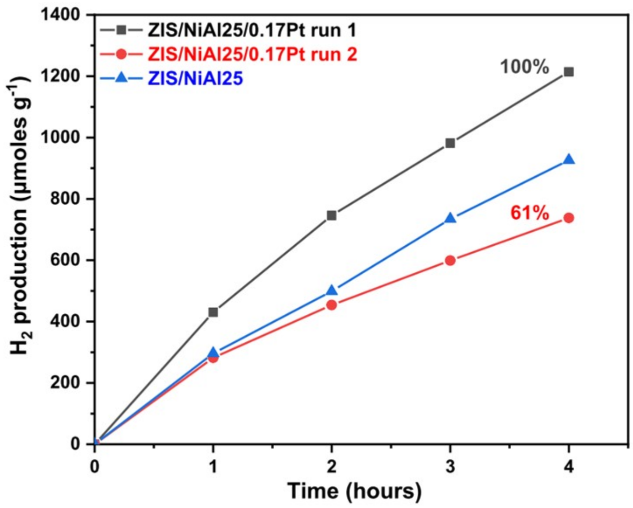

Figure S12. Cycling study of ZIS/NiAl/0.17Pt under visible irradiation (λ>420 nm). Reaction conditions: 25 mg of catalyst, 20 mL aqueous solution, 10% v/v of sacrificial agent (TEOA), Xe lamp 1000Watt

Table S2: The values of obtained AQE(%) in different wavelengths

λ (nm)	AQE (%)
320	1.70
350	1.40
420	0.30
450	0.10
500	0.02
600	0.03

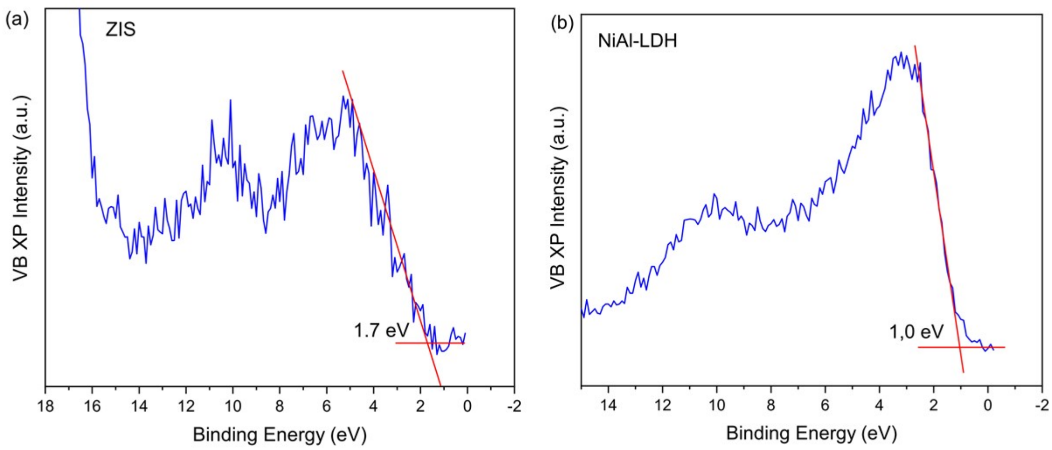

Figure S13. Valence band XP spectra of (a) ZIS and (b) NiAl-LDH samples.

References:

[1] P. Kalisman, Y. Nakibli, and L. Amirav, "Perfect Photon-to-Hydrogen Conversion Efficiency," *Nano Lett.*, vol. 16, no. 3, pp. 1776–1781, 2016, doi: 10.1021/acs.nanolett.5b04813.

[2] X. Deng *et al.*, "Carbon-Dots-Modified Hierarchical $ZnIn_2S_4$/Ni-Al LDH Heterojunction with Boosted Charge Transfer for Visible-Light-Driven Photocatalytic H2 Evolution," *Inorg. Chem.*, vol. 62, no. 24, pp. 9702–9712, 2023, doi: 10.1021/acs.inorgchem.3c01317.

[3] S. Zhao *et al.*, "In Situ Growth of $ZnIn_2S_4$ on MOF-Derived Ni-Fe LDH to Construct Ternary-Shelled Nanotubes for Efficient Photocatalytic Hydrogen Evolution," *Inorg. Chem.*, vol. 60, no. 13, pp. 9762–9772, 2021, doi: 10.1021/acs.inorgchem.1c01064.

[4] Z. Yang, S. Li, X. Xia, and Y. Liu, "Hexagonal MgAl-LDH simultaneously facilitated active facet exposure and holes storage over $ZnIn_2S_4$/MgAl-LDH heterojunction for boosting photocatalytic activities and anti-photocorrosion," *Sep. Purif. Technol.*, vol. 300, no. July, p. 121819, 2022, doi: 10.1016/j.seppur.2022.121819.

[5] Z. He, C. Qian, D. Chen, K. Xu, and W. Hao, "Design of ultrathin CoAl-LDHs/ $ZnIn_2S_4$ with strong interfacial bonding and rich oxygen vacancies for highly efficient hydrogen evolution activity," *J. Colloid Interface Sci.*, vol. 651, no. July, pp. 138–148, 2023, doi: 10.1016/j.jcis.2023.07.179.

[6] D. Wang, Z. Yang, Y. Xie, Y. Feng, and J. Yao, "NiCo Layered Double Hydroxide Bearing $ZnIn_2S_4$ anosheets for Highly Efficient Photocatalytic Cr(VI) Reduction," *ACS Appl. Nano Mater.*, vol. 6, no. 7, pp. 6086–6091, 2023, doi: 10.1021/acsanm.3c00427.

[7] L. Peng *et al.*, "Self-assembled transition metal chalcogenides@CoAl-LDH 2D/2D heterostructures with enhanced photoactivity for hydrogen evolution," *Inorg. Chem. Front.*, vol. 9, no. 5, pp. 994–1005, 2022, doi: 10.1039/d1qi01603b.

[8] C. Tang *et al.*, "Bioinspired 3D penetrating structured micro-mesoporous NiCoFe-LDH@ $ZnIn_2S_4$ Z-scheme heterojunction for simultaneously photocatalytic H_2 evolution coupled with benzylamine oxidation," *Appl. Catal. B Environ.*, vol. 342, no. September 2023, 2024, doi: 10.1016/j.apcatb.2023.123384.

[9] Q. Zhou, B. Jiang, L. Zhang, Y. Sun, X. Yang, and L. Zhang, "1D/2D CoNi-LDH/ $ZnIn_2S_4$ S-scheme heterojunction for effectively tetracycline degradation under photocatalytic-peroxymonosulfate activation system: DFT calculations and mechanism insights," *Chem. Eng. J.*, vol. 478, no. August, p. 147535, 2023, doi: 10.1016/j.cej.2023.147535.